https://doi.org/10.5194/egusphere-2025-1785
Preprint. Discussion started: 30 April 2025

Model Predictive Control with Foreseeing Horizon Designed to Mitigate Extreme Events in Chaotic Dynamical Systems

Fumitoshi Kawasaki[1], Atsushi Okazaki[2,3], Kenta Kurosawa[2], Tadashi Tsuyuki[2,4], Shunji Kotsuki[2,3,5]

[1]Graduate School of Science and Engineering, Chiba University, Chiba, Japan
[2]Center for Environmental Remote Sensing, Chiba University, Chiba, Japan
[3]Institute for Advanced Academic Research, Chiba University, Chiba, Japan
[4]Meteorological Research Institute, Japan Meteorological Agency, Tsukuba, Japan
[5]Research Institute of Disaster Medicine, Chiba University, Chiba, Japan

Correspondence to: Fumitoshi Kawasaki (fkawasaki@chiba-u.jp) and Shunji Kotsuki (shunji.kotsuki@chiba-u.jp)

Abstract. Practical applications of weather control are being explored under Japan's Moonshot Research and Development Program to mitigate extreme weather events such as heavy rainfall. One of the most significant challenges in this endeavor is identifying effective and efficient control inputs to mitigate extreme weather events within limited energy and computational time. To address this difficulty, the development of mathematical weather control approaches is being promoted. However, further improvements to the conventional approaches are required for the practical applications of weather control. In this study, we propose a novel framework called model predictive control with foreseeing horizon (MPCF), designed to mitigate extreme events in chaotic dynamical systems. The MPCF aims to improve control effectiveness by leveraging the sensitivity to initial conditions of chaotic dynamical systems. We evaluated the MPCF through control simulation experiments using the Lorenz 96 model. Our results demonstrated that introducing the foreseeing horizon improved the success rate without substantially increasing the computational cost of optimization, particularly when the control horizon was short. Furthermore, a comparison with the conventional method showed that the MPCF achieved success rates comparable to the conventional method with lower computational costs. This study showed that the MPCF is a promising control framework for mitigating extreme events in chaotic dynamical systems.

1 Introduction

Anthropogenic climate change is raising concerns about the increased frequency and intensity of extreme events, including heavy rainfall, around the world. To avoid these weather-related disasters, warnings and evacuations based on numerical weather prediction (NWP) have been conducted together with the development of disaster prevention infrastructure including dams and levees. However, such passive countermeasures for weather-related disasters alone have their limitations. To overcome these limitations, Japan's Moonshot Research and Development Program is being promoted to develop weather control technologies for mitigating extreme events through intentional interventions. For example, to mitigate torrential rainfall, a strategy is being explored to reduce the amount of water vapor flowing to land by artificially inducing the self-organization

https://doi.org/10.5194/egusphere-2025-1785
Preprint. Discussion started: 30 April 2025

of the meso-convective systems over the ocean using intervention technologies, including cloud seeding and atmospheric heating (Kotsuki, 2024). However, there are various challenges in realizing the mitigation of extreme weather events. One of the most significant difficulties is identifying effective and efficient control inputs to mitigate extreme events with limited energy and computational time. To solve these problems, the development of mathematical weather control approaches for identifying the control inputs is indispensable. In contrast to widely explored control problems, we consider that weather control approaches are required to satisfy the following three key characteristics:

1. Optimality: identifying optimal control inputs to mitigate extreme events in chaotic dynamical systems with strong nonlinearities.
2. Restrictiveness: constraining control inputs within feasible magnitudes.
3. Rapidity: computing control inputs rapidly in real time.

Miyoshi and Sun (2022) proposed a simple approach utilizing the sensitivity to initial values of chaotic dynamical systems in a control simulation experiment (CSE), which is an experimental framework for evaluating controllability as an extension of the observing system simulation experiment (OSSE). Specifically, this approach nudges the initial values of a chaotic dynamical system toward those of an ensemble member forecasting a desirable regime. To do so, the difference vector between two ensemble members—one exhibiting a desirable regime and the other an undesirable regime—is used as control inputs (hereafter referred to as the difference-based approach). Miyoshi and Sun (2022) demonstrated that the difference-based approach successfully led the Lorenz 63 system (Lorenz, 1963) to the prescribed regime. Sun et al. (2023) investigated the properties of parameters such as localization in the CSE and found that localized control inputs reduced the intervention cost without significantly compromising controllability using the Lorenz 96 model (L96; Lorenz, 1996). Ouyang et al. (2023) improved the difference-based approach by utilizing the growth rate of singular vectors and succeeded in reducing the total magnitude of control inputs with the Lorenz 63 model. Subsequently, Kawasaki and Kotsuki (2024) proposed using model predictive control (MPC), an advanced nonlinear control method explored in the control engineering field, within the CSE. MPC can perform optimization while satisfying constraints based on a cost function with penalty terms. Indeed, Kawasaki and Kotsuki (2024) succeeded in leading the Lorenz 63 system to the prescribed regime while satisfying constraints of the norm of the control input. Afterwards, Sawada (2024) proposed ensemble Kalman control (EnKC), which uses an ensemble Kalman filter (EnKF; Evensen, 1994) to approximately reduce the cost function of MPC. In the EnKC, pseudo observations are generated around the desirable regime. By assimilating these pseudo observations, the system would be guided toward the desirable regime, with the analysis increments acting as control inputs. Sawada (2024) demonstrated that the EnKC successfully led the Lorenz 63 system to the prescribed regime, in line with previous CSE studies.

Each of these approaches has contributed valuable insights, although there remains room for further development. Among them, an approach using MPC would be particularly promising for future practical weather control applications. We highlight the rationale behind this assessment in terms of the optimality, restrictiveness, and rapidity, as summarized in Table 1. The difference-based approach is straightforward and easily implemented; however, it currently lacks an optimization process. Furthermore, explicitly constraining the norm of the control input poses a significant challenge. While it is certainly possible

https://doi.org/10.5194/egusphere-2025-1785
Preprint. Discussion started: 30 April 2025

to scale the norm to a certain value, doing so may compromise optimality. Therefore, the difference-based approach has limitations regarding its optimality and restrictiveness. One major advantage of the EnKC is that it can leverage existing ensemble data assimilation (DA) schemes with almost no modifications for algorithm implementation of control problems. However, the EnKC relies on ensemble approximation; therefore, it has a limitation in optimality. Additionally, the EnKC, an approach based on a DA method, inherently calculates a control input only at the initial time of a DA window, limiting its flexibility compared to MPC, which can manage multiple-step control inputs. It is certainly possible to divide the control inputs at the initial time into several time steps, akin to the incremental analysis update (IAU; Bloom et al., 1996) method used in DA, but this is suboptimal (Sawada, 2024). Furthermore, the EnKC faces a significant limitation in terms of the restrictiveness. Even if control inputs could be constrained in ensemble space, the EnKC would not be able to constrain them in model space. This is because the ensemble perturbation matrix must be applied to map from ensemble space to model space, rendering control input constraints in model space unenforceable. Therefore, the EnKC has limitations in terms of both optimality and restrictiveness, thereby sharing similar constraints with the difference-based approach. The conventional MPC, on the other hand, can optimize control inputs under constraints, thus satisfying both the optimality and restrictiveness. In addition, MPC is similar to variational DA methods in which the cost function is minimized within a certain time interval through iterative computations (Sawada, 2024). Therefore, given the analogy with variational DA methods, the operational success of four-dimensional variational data assimilation (4DVar; Dimet and Talagrand, 1986; Talagrand and Courtier, 1987) and four-dimensional ensemble-based variational data assimilation (4DEnVar; Zupanski, 2005; Liu et al., 2008) would support the potential effectiveness of MPC. Actually, these variational DA methods are widely used in major NWP centers such as the European Centre for Medium-Range Weather Forecasts (ECMWF), the United Kingdom Met Office (Met Office), the National Oceanic and Atmospheric Administration of the United States (NOAA), and the Japan Meteorological Agency (JMA). On the other hand, the conventional MPC suffers from computational inefficiencies due to the iterative optimization required to identify control inputs. However, there is significant potential for methodological improvements in MPC to reduce computational time, such as by incorporating artificial intelligence (AI) weather prediction models.

In this study, we propose a novel MPC framework designed to mitigate extreme events in chaotic dynamical systems: model predictive control with foreseeing horizon (MPCF). By incorporating the innovative concept of a foreseeing horizon, the MPCF can detect extreme events earlier than the conventional MPC, enabling proactive control strategies. Consequently, we assume that leveraging the sensitivity to initial conditions inherent in chaotic dynamical systems can facilitate easier control, thereby reducing computational cost. To evaluate the proposed method, we conducted a series of CSEs with the 40-variable L96, a simplified atmospheric model, as the next step of the Lorenz 63 model (Kawasaki and Kotsuki, 2024). Specifically, we first defined extreme events in the L96 according to Sun et al. (2023), and subsequently performed statistical evaluations of the MPCF.

The remainder of this paper is structured as follows. Section 2 introduces the MPCF. Section 3 describes the experimental design of the CSEs with the L96. In Sect. 4, we present and discuss the results of the CSEs. Finally, Sect. 5 presents a summary.

https://doi.org/10.5194/egusphere-2025-1785
Preprint. Discussion started: 30 April 2025

Table 1: Characteristics of the current major control approaches for control simulation experiments.

Control approaches	Optimality	Restrictiveness	Rapidity
Difference-based approach	Not satisfied	Not satisfied	Satisfied
EnKC	Partially satisfied	Not satisfied	Partially satisfied
Conventional MPC	Satisfied	Satisfied	Not satisfied
MPCF (this study)	Satisfied	Satisfied	Partially satisfied

2 Methodology

2.1 Model predictive control

In this study, we extend the conventional MPC to the MPCF, and subsequently compare their performances in CSEs. The core concept of MPC is to perform optimal control at each time, taking into account the anticipated future states and control inputs from the current time. The concise procedure of MPC is described as follows (Fig. 1).

1. Prediction and optimization step: at time t_i, the prediction horizon T_p and control horizon T_c are set, where T_p represents the length of state prediction and T_c ($T_\mathrm{c} \leq T_\mathrm{p}$) represents the length of the control inputs to be optimized. Note that a new axis τ is introduced as the time axis for both horizons (i.e., $\tau = 0$ denotes the initial times of both horizons) and is set to be independent of the time axis t. Then, the prediction of state $\boldsymbol{x}^*(\tau; t)$ from $\tau = 0$ to $\tau = T_\mathrm{p}$ and optimization of control input $\boldsymbol{u}^*(\tau; t)$ from $\tau = 0$ to $\tau = T_\mathrm{c}$ are iteratively performed to minimize a cost function designed to achieve desirable control results. Here, $\boldsymbol{x}^*(\tau; t)$ and $\boldsymbol{u}^*(\tau; t)$ denote the state and control input at time axis τ of the horizon at time axis t, respectively. The superscript "$*$" denotes variables over the horizons.
2. Addition of control inputs and time evolution: an extracted segment of time interval $(0, \tau_i)$ where $\tau_i \leq T_\mathrm{c}$ from $\boldsymbol{u}^*(\tau; t)$ is used as the control input $\boldsymbol{u}(t)$ to be actually added to the state. Then, $\boldsymbol{u}(t)$ is added to the state $\boldsymbol{x}(t)$**,** and $\boldsymbol{x}(t)$ is evolved in time.

The cost function of MPC depends on the control purpose, but a general formulation is expressed by:

$$J = \sum_{\tau=0}^{T_\mathrm{c}-1} J_{\boldsymbol{u}}\left(\boldsymbol{u}^*(\tau; t)\right) + \sum_{\tau=0}^{T_\mathrm{p}} J_{\boldsymbol{x}}\left(\boldsymbol{x}^*(\tau; t)\right). \tag{1}$$

Note that in Kawasaki and Kotsuki (2024), the cost function was minimized by solving the Euler–Lagrange equation, but in this study, the cost function is minimized directly using the quasi-Newton method. This distinction can be understood by drawing an analogy with the historical evolution of DA. The 4DVar prototype originally studied by Sasaki (1969, 1970) and Thompson (1969) solved the Euler–Lagrange equation. However, solving the Euler–Lagrange equation for large-dimensional problems such as the atmosphere is difficult (Tsuyuki and Miyoshi, 2007). Accordingly, a more efficient adjoint method was introduced by Dimet and Talagrand (1986) and Talagrand and Courtier (1987). Many operational models employing

https://doi.org/10.5194/egusphere-2025-1785
Preprint. Discussion started: 30 April 2025

variational DA now use the adjoint method. Therefore, the adjoint method would also be suitable in the application of MPC to large-dimensional systems such as the atmosphere.

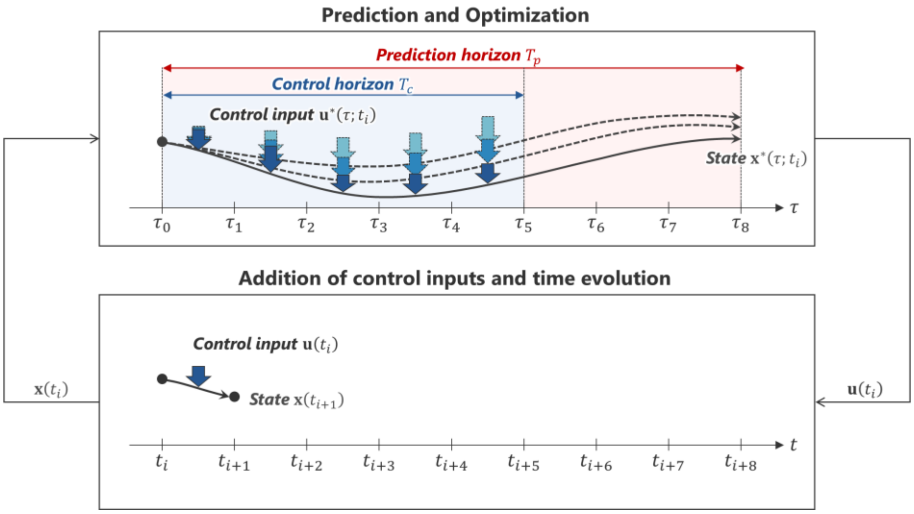

Figure 1: The concept of MPC. Prediction of state $\boldsymbol{x}^*(\tau; t)$ in the predictive horizon T_p and optimization of control input $\boldsymbol{u}^*(\tau; t)$ in the control horizon T_c are performed iteratively (upper box). The segment extracted from $\boldsymbol{u}^*(\tau; t)$ is used as the control input $\boldsymbol{u}(t)$ to be actually added to the state $\boldsymbol{x}(t)$. Then, $\boldsymbol{u}(t)$ is added to the state $\boldsymbol{x}(t)$ in the time evolution (lower box), followed by the next time t_{i+1}.

2.3 Model predictive control with foreseeing horizon

2.3.1 Concept of MPCF

The MPCF proposed in this study is an MPC framework designed to mitigate extreme events in chaotic dynamical systems. Specifically, MPCF introduces the new concept, the foreseeing horizon T_f, in addition to the control horizon T_c and prediction horizon T_p. To reduce the computational cost and intervention energy, conventional CSE studies have employed a control framework that only activates control when a forecasted ensemble member indicates a non-desirable regime. Kawasaki and Kotsuki (2024) employed a control design that set the length of this ensemble forecast equal to the length of T_p. However, the problem whereby extending T_p would greatly increase the computational cost for identifying control inputs remained. Accordingly, we consider that T_f, the length of the ensemble forecast used to judge whether to activate the control or not, should be set independently from T_p. Thereby, it would be possible to detect extreme events earlier without a significant increase in computational cost. Furthermore, by detecting extreme events earlier, it is expected that control with small control inputs and low computational cost can be achieved by effectively utilizing the sensitivity to initial conditions in chaotic dynamical systems.

https://doi.org/10.5194/egusphere-2025-1785
Preprint. Discussion started: 30 April 2025

2.3.2 The MPCF procedure in the CSE

The CSE is an experimental control framework for chaotic dynamical systems proposed by Miyoshi and Sun (2022). The concept of the CSE is that the values of the nature run (NR) are unknown, but interventions can be added to the NR as for the real atmosphere. Note that the DA process is essential in the CSE, unlike an ordinary control simulation, because the CSE is generally intended for chaotic dynamical systems.

The MPCF procedure in the CSE is described as follows using Fig. 2.

1. DA and ensemble forecast (Fig. 2, a): At time t_i, the EnKF performs DA to provide an analysis ensemble $\mathbf{X}^{\mathrm{a}}$. Subsequently, an ensemble forecast is computed for the foreseeing horizon T_{f} from $\mathbf{X}^{\mathrm{a}}$. If an extreme event is detected during the ensemble forecast, the control is activated, and the process continues to step 2. Otherwise, the process goes to step 3 with no control input.
2. Tracking the reference trajectory (Fig. 2, b): The trajectory of an ensemble member showing a non-disastrous regime within the ensemble forecast is set as the reference trajectory $\boldsymbol{x}^{\mathrm{r}}$. The control inputs for tracking the reference trajectory are identified through optimization. Here, the difference between the true state and the initial state used for computing the control inputs is the main source of uncertainty in the control results.
3. Addition of the control inputs and simulation of observations (Fig. 2, c): A segment of the control input $\boldsymbol{u}(t_i)$ until the next observation time t_{i+o} from the identified control input $\boldsymbol{u}^*(\tau; t)$ is added to the NR and the forecast ensemble $\mathbf{X}^{\mathrm{b}}$, and the NR and $\mathbf{X}^{\mathrm{b}}$ are integrated to the next observation time t_{i+o}. Here, o is the time interval of the observation. Note that if step 2 is skipped, no control input is added. Subsequently, observation $\boldsymbol{y}^{\mathrm{o}}$ is simulated by adding random numbers to the NR.
4. Continuation or discontinuation of reference trajectory tracking (Fig. 2, d): At the next observation time t_{i+o}, DA and ensemble forecast are performed until $t_i + T_f$. If an extreme event is detected, the tracking to the reference trajectory is continued as in step 2 using $\boldsymbol{x}^{\mathrm{r}}$ set at time t_i (i.e., without resetting the reference trajectory), and the process proceeds to steps 3 and 4. If not, tracking to the reference trajectory is deactivated, and the process goes to step 1. This is because if the NR rides on the non-disastrous attractor once, the activated control should not be needed.

https://doi.org/10.5194/egusphere-2025-1785
Preprint. Discussion started: 30 April 2025

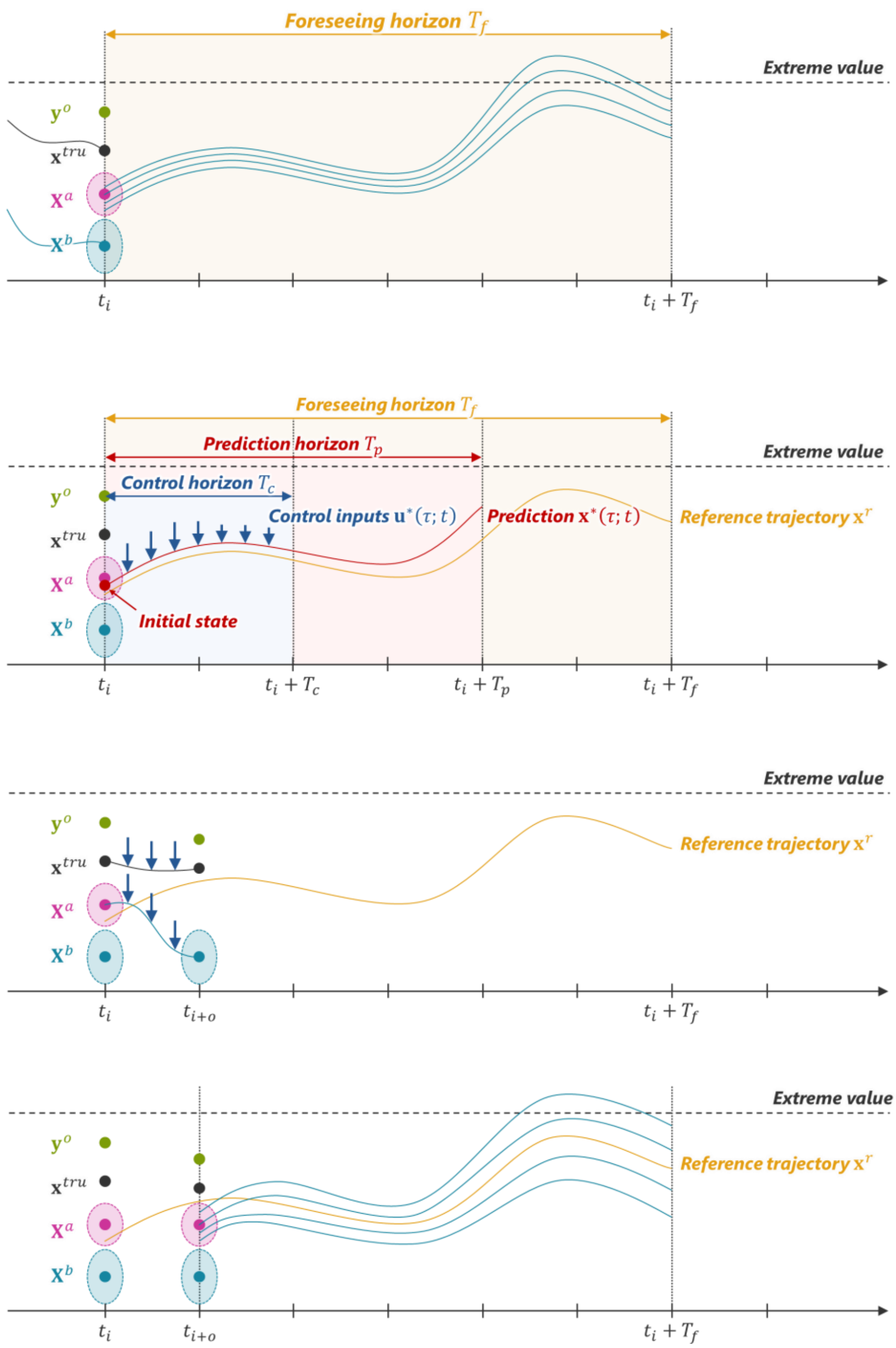

Figure 2: The MPCF procedure. (a) DA and ensemble forecast for the foreseeing horizon T_f are performed (step 1). (b) Tracking the reference trajectory is achieved by predicting state $\boldsymbol{x}^*(\tau; t)$ and optimizing control input $\boldsymbol{u}^*(\tau; t)$ iteratively (step 2). (c) The segment of control input $\boldsymbol{u}(t)$ is added, and observation $\boldsymbol{y}^\mathrm{o}$ is simulated around the NR (step 3). (d) It is judged whether to continue or discontinue the reference trajectory tracking (step 4).

https://doi.org/10.5194/egusphere-2025-1785
Preprint. Discussion started: 30 April 2025

3 Experimental designs

3.1 The Lorenz 96 model

In this study, the CSEs are performed using the L96, a chaotic dynamical system formulated by Lorenz (1996), following Sun et al. (2023). The equation of the L96 is expressed as a differential equation with advection, dissipation, and forcing terms that are intrinsic to the weather phenomenon, as follows:

$$\frac{\mathrm{d}X_i}{\mathrm{d}t} = (X_{i+1} - X_{i-2})X_{i-1} - X_i + F \tag{2}$$

for $i = 0, \cdots, k$ and $k = 39$ (i.e., the number of model variables is $n = 40$) in this study. In addition, the value of the forcing term is set to $F = 8.0$ for the model to behave chaotically. Note that the L96 is assumed to have a periodic boundary condition (i.e., $X_{-1} = X_k$ and $X_0 = X_n$). The variables in the L96 are interpreted as certain physical quantities equally distributed on the same latitude circle (Lorenz and Emanuel, 1998).

This study discretizes and integrates the L96 using the fourth-order Runge–Kutta scheme. One time step of integration is defined as $\mathrm{d}t = 0.01$ non-dimensional unit of time throughout this study. In the L96 with $F = 8.0$, one unit of time is equivalent to 5 d (i.e., $\mathrm{d}t = 0.01$ unit of time is equivalent to 1.2 hours) following a discussion of error doubling time by Lorenz and Emanuel (1998).

Note that when a control input u_k is added to the state variable X_i, the equation of the L96 is expressed as:

$$\frac{\mathrm{d}X_i}{\mathrm{d}t} = (X_{i+1} - X_{i-2})X_{i-1} - X_i + F + u_i. \tag{3}$$

Namely, control inputs are added through the model time integration rather than directly to change states in this study. Therefore, the values of the control inputs presented in this study cannot be directly compared to the values of the states. Multiplying this value by $\mathrm{d}t$ is equivalent to the value of the control input in the case of direct addition to the state.

3.2 The EnKF

Here, the EnKF used in the CSEs of this study is described. This study assumes a large ensemble size and employs an ensemble size of 200 to obtain better reference trajectories for the MPCF. With respect to the EnKF, it is known that stochastic filters are more robust against nonlinearity than deterministic filters when sufficient ensemble size is available (Lawson and Hansen, 2004). Therefore, this study employs the perturbed observation (PO) method (Burgers et al., 1998) as the EnKF used in the CSEs. For simplicity, multiplicative inflation is employed as covariance inflation for background ensemble perturbations with a manually tuned optimal inflation factor of 1.06.

3.3 The MPCF

In this study, the following cost function is used for the MPCF:

$$J = \sum_{i=0}^{T_\mathrm{c}-1} \frac{1}{2} w \cdot \{\max(\|\boldsymbol{u}_i^*\| - U_{\max},\ 0)\}^2 + \sum_{i=0}^{T_\mathrm{p}} \frac{1}{2} (\boldsymbol{x}_i^\mathrm{r} - \boldsymbol{x}_i^*)^T \mathbf{W} (\boldsymbol{x}_i^\mathrm{r} - \boldsymbol{x}_i^*), \tag{4}$$

https://doi.org/10.5194/egusphere-2025-1785
Preprint. Discussion started: 30 April 2025

where the first term has the effect of constraining the norm of the control input (i.e., a penalty term), and the second term represents the tracking of the reference trajectory. The vector $\boldsymbol{u}_i^* \in \mathbb{R}^l$ is the control input of the i-th step in the control horizon T_c, and the vectors $\boldsymbol{x}_i^*, \boldsymbol{x}_i^\mathrm{r} \in \mathbb{R}^n$ are the prediction of state and the reference trajectory of the i-th step in the prediction horizon T_p, respectively. The scalar $U_\mathrm{max} \in \mathbb{R}$ is the value that the norm of the control input is constrained to. The scalar $w \in \mathbb{R}$ and the diagonal matrix $\mathbf{W} \in \mathbb{R}^{n\times n}$ are penalty parameters. These tunable parameters impose large penalties when the constraints are not satisfied and play a role in adjusting the balance between these constraints. In addition, a diagonal matrix $\mathbf{W}$ determines the weights for tracking the reference trajectories at each grid point. From our preliminary experiments, $w = 10^4$, and $\mathbf{W}$ is determined to be 1.0 for only the i-th diagonal component corresponding to the target point X_i of the extreme event mitigation. In addition, the Broyden–Fletcher–Goldfarb–Shanno (BFGS) algorithm (an option of the scipy.optimize.minimize tool in the SciPy library) is used for minimization of the cost function. See Appendix A for details on how to select the reference trajectory and the initial state used in optimization.

3.4 The CSE

3.4.1 Preparation

Here, we explain how to generate the NR, forecast ensemble, and analysis ensemble for use at the beginning points of the CSEs. First, the 22-year NR is conducted with the L96. The initial values of the NR are generated by random numbers $\mathcal{N}(0.0, 1.0)$ following the Gaussian distribution for 40 variables independently. The first year of the 22-year NR is discarded for the spin up. Observations are generated at all grid points every 0.05 units of time (i.e., 5 steps) by adding noise following the Gaussian distribution $\mathcal{N}(0.0, 1.0)$ to the NR and applying the observation operator which is an identity matrix. The DA cycles are performed for 21 years using the PO method for generating the forecast and analysis ensembles. The initial values of the forecast ensemble are generated by adding noise following the Gaussian distribution $\mathcal{N}(0.0, 1.0)$ to the NR, as in the observations. The observation error covariance matrix is set to the identity matrix. We discard the first year of the 21-year DA cycles to eliminate poor-quality analysis ensembles. Along with this, the first year of the NR is discarded. Thus, 20 years of the NR, the forecast ensemble, and the analysis ensemble are used as the data for the CSEs.

Subsequently, we define the threshold of extreme events in the L96 like Sun et al. (2023). First, the average of the top 40 local maxima over a 6-h period at each grid point in the 20-year NR is defined as the threshold of extreme events. The reason for storing the local maxima over a 6-h period is to prevent counting only the values in a short interval around the global maximum. As a result, an extreme event appears twice a year at each grid point statistically. The threshold of extreme events is defined as 12.16 in this study.

https://doi.org/10.5194/egusphere-2025-1785
Preprint. Discussion started: 30 April 2025

3.4.2 Statistical evaluation

In Sect. 4, we present the result obtained using the MPCF. We begin by showcasing an exemplary result of the MPCF in Sect. 4.1, followed by a series of statistical evaluations in Sects. 4.2-4.4 (Table 2). Specifically, Sect. 4.2 explores the sensitivity to the control, prediction, and foreseeing horizons. Section 4.3 examines the sensitivity to the constrained norm of the control input. Finally, Sect. 4.4 investigates the sensitivity to the placement of the control input.

For a fair statistical evaluation, a single CSE is designed so that only one extreme event appears at the targeted point X_i. In addition, a CSE is started 14 d before the time of the target extreme event in the generated 20-year data, and the behavior is monitored until 7 d after the time of the target extreme event. In this study, extreme events appearing at 20 grid points of X_i $(i = 0, 2, 4, \cdots, 38)$ are subject to statistical evaluation. A total of 193 samples of extreme events are obtained for the 20 grid points, as a result of the selection to satisfy the extreme event criteria and to ensure that only one extreme event appears per CSE. Therefore, the evaluation results of this study are the statistics over these 193 samples. Note that the results are statistically equivalent at any grid points because the L96 has the periodic boundary condition.

In this study, the success rate (SR), the mean maximum control input (MMCI), and the mean one-time optimization time (MOOT) are introduced as evaluation indicators. The SR indicates the rate of cases avoiding extreme events among the 193 results. The MMCI represents the maximum norm of the control input in a CSE averaged over 193 cases. The MOOT expresses the mean computational time for one optimization of the cost function averaged over all MPC computations of 193 cases. Each CSE uses four processing cores in DELL PowerEdge R6525 servers, equipped with dual AMD EPYC 7352 processors.

https://doi.org/10.5194/egusphere-2025-1785
Preprint. Discussion started: 30 April 2025

Table 2: Summary of the settings for each experiment.

Experiment	Placement of control inputs	Control horizon T_c	Prediction horizon T_p	Foreseeing horizon T_f	The constrained norm of the control input U_max
Sect. 4.1	X_{37}, X_{38}, X_{39}	6 h	24 h	96 h	2.0
Sect. 4.2	X_{i-1}, X_i, X_{i+1}	$6, 12, 24, 48, 96, 168$ h	$6, 12, 24$ h	$48, 96, 168$ h	2.0
Sect. 4.3	X_{i-1}, X_i, X_{i+1}	6 h	24 h	96 h	$1.0, 2.0, 4.0, 7.0, 14$
Sect. 4.4	$X_{i-2}, X_{i-1}, X_i,$ X_{i+1}, X_{i+1} $(X_{i-3}, X_{i-2}, X_{i-1}),$ $(X_{i-2}, X_{i-1}, X_i),$ $(X_{i-1}, X_i, X_{i+1}),$ $(X_i, X_{i+1}, X_{i+2}),$ $(X_{i+1}, X_{i+2}, X_{i+3})$	6 h	24 h	96 h	2.0

4 Results and discussion

4.1 An example result of the CSE

This experiment confirms how the controlled NR and control inputs behave with the MPCF. In this experiment, an arbitrarily selected extreme event appearing in X_{38} is targeted, and control inputs are added to X_{37}, X_{38}, and X_{39}. The control, prediction, and foreseeing horizons are set to $T_\mathrm{c} = 6$, $T_\mathrm{p} = 24$, and $T_\mathrm{f} = 96$ h, respectively. The constrained norm of the control input is set to $U_\mathrm{max} = 2.0$.

The NR and the controlled NR of X_{38} are shown in Fig. 3 (a). The figure shows that the NR without control (gray solid line) exceeds the threshold of extreme events (black dotted horizontal line), whereas the extreme event of the controlled NR (black solid line) is successfully mitigated by tracking the reference trajectory (red and blue solid lines) with the MPCF. Specifically, the first reference trajectory (red solid line) is set at -4.75 d (red shade, cf. step 2 in Sect. 2.3.2). The NR is controlled to track the reference trajectory until -2.75 d (over yellow shade) by the MPCF as no extreme event is forecasted up to $t = -4.75 + T_\mathrm{f}/24$ d (cf. step 4 in Sect. 2.3.2). However, an extreme event is forecasted within $-2.75 + T_\mathrm{f}/24$ d at $t = -2.75$ d; therefore, the second reference trajectory is newly set (blue solid line). The blue reference trajectory is then tracked in the same way, and tracking the reference trajectory is interrupted at $t = -0.5$ d (at the end of green shade). After this time, the NR avoids the

https://doi.org/10.5194/egusphere-2025-1785
Preprint. Discussion started: 30 April 2025

extreme event without control because it is on a non-disastrous attractor. The control inputs in X_{37}, X_{38}, X_{39}, and their norm are shown in Fig. 3 (b−e), respectively. While each control input shows a complex signal, the norm of the control input is successfully constrained below $U_{\max}$, as represented by the black dotted line in Fig. 3 (e). Therefore, the MPCF successfully mitigates the extreme event while constraining the norm of the control input in this case.

285

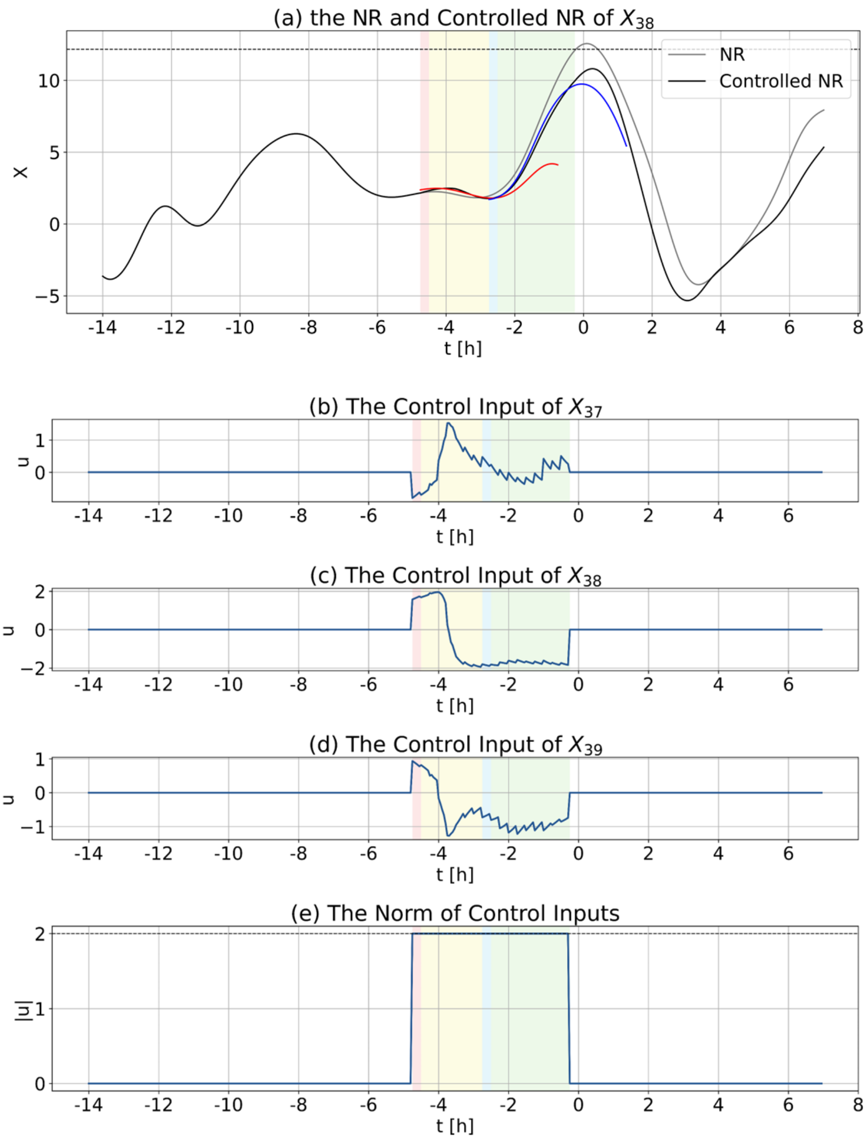

Figure 3: An example of mitigating the extreme event at X_{38} in the L96 by the MPCF. (a) The NR (gray solid line) and the controlled NR (black solid line) of X_{38} in the L96 by the MPCF. The threshold of extreme events is shown by the black
290 horizontal dotted line. The red and blue solid lines are the first and second reference trajectories, which are set and tracked at

https://doi.org/10.5194/egusphere-2025-1785
Preprint. Discussion started: 30 April 2025

the times of the red and blue shades, and the reference trajectories are tracked over the times of the yellow and green shades. (b–d) The control inputs in X_{37}, X_{38}, and X_{39}, respectively. (e) The norm of the control input. The black dotted line in (e) indicates the constrained norm of the control input U_{max}.

4.2 Sensitivity to the control, prediction, and foreseeing horizons

In this experiment, we investigate the sensitivity to the control, prediction, and foreseeing horizons, T_{c}, T_{p}, and T_{f}, respectively. The placement of the control input is X_{i-1}, X_i, and X_{i+1}, and the constrained norm of the control input is $U_{\mathrm{max}} = 2.0$. To investigate the sensitivity, the control horizon is set to $T_{\mathrm{c}} = 6$, 12, and 24 h, the prediction horizon is set to $T_{\mathrm{p}} = 6$, 12, 24, 48, 96, and 168 h, and the foreseeing horizon is set to $T_{\mathrm{f}} = 48$, 96, and 168 h.

The statistical results are shown in Fig. 4. The deeper colors in Fig. 4 represent better outcomes. Initially, let us focus on the T_{c} axis. Across all cases, the SR hardly improves by extending T_c, while the MOOT increases sharply. The MMCI remains largely unchanged. That is, there is no significant effect of extending T_{c} longer than the observation time of 6 h. Subsequently, focusing on the T_{p} axis, the SR improves overall by extending T_{p}. On the other hand, the MOOT increases by extending T_{p}, although not as much as for extending T_{c}. In addition, although it is acceptable, extending T_{p} may cause the MMCI to slightly exceed U_{max}. This is because extending T_{p} increases the costs of tracking the reference trajectory and relatively reduces the effect of constraining the norm of the control input to U_{max} (cf. Eq. 4). Therefore, this problem would be solved by calibrating the penalty parameters. Finally, focusing on the T_{f} direction, the SR improves without significant changes to the MMCI and MOOT by extending T_{f}, especially when T_{c} is short. We consider that this is because extreme events can be detected earlier by introducing the T_{f}, and the sensitivity to initial conditions of the L96 is effectively utilized.

Here, the result of a comparison between the conventional MPC (i.e., $T_{\mathrm{p}} = T_{\mathrm{f}}$) and the MPCF (i.e., $T_{\mathrm{p}} < T_{\mathrm{f}}$), using the results for $T_{\mathrm{c}} = 6$ h is shown in Fig. 5. This result indicates that the MPCF (yellow dots) can achieve SRs almost equivalent to those of the conventional MPC (red dots) with lower MOOTs. For example, when the SR is approximately 0.75 to 0.76, the MOOT of the conventional MPC is 56.5 s, whereas that of the MPCF is significantly reduced to 13.5 s. In conclusion, the MPCF is a promising approach for mitigating extreme events in chaotic dynamical systems with lower computational costs than the conventional MPC.

https://doi.org/10.5194/egusphere-2025-1785
Preprint. Discussion started: 30 April 2025

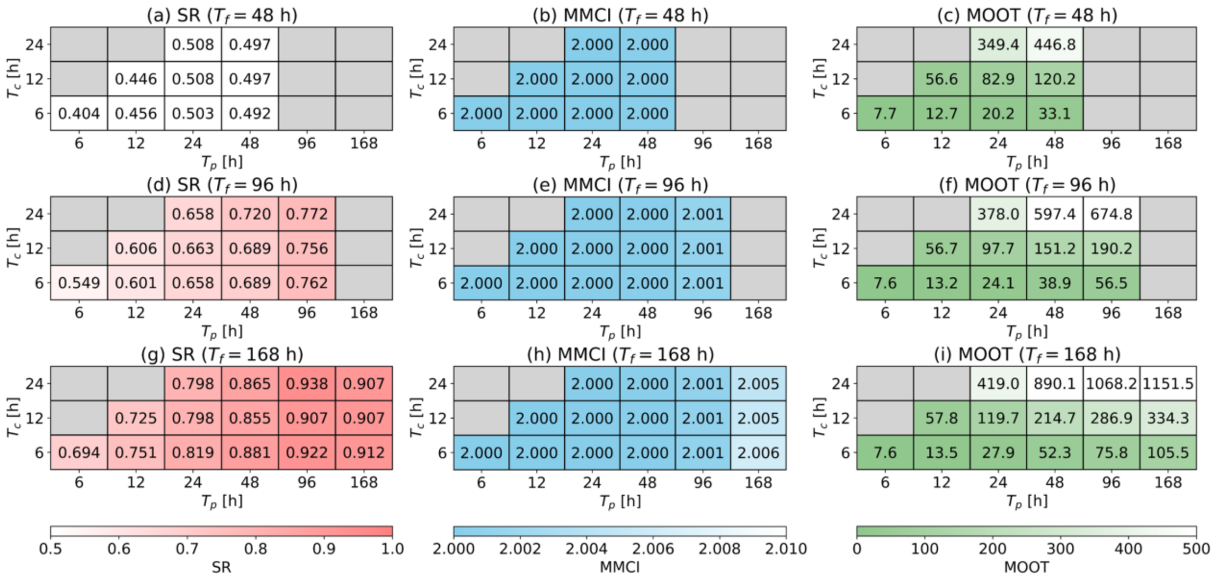

Figure 4: Sensitivity to the control, prediction, and foreseeing horizons, T_c, T_p, and T_f, respectively, based on three indicators: the success rate (SR), the mean maximum control input (MMCI), and the mean one-time optimization time
320 (MOOT). In each heat map, the horizontal axis is T_p and the vertical axis is T_c. (a–c) are the results for $T_f = 48$ h, (d–f) are the results for $T_f = 96$ h, and (g–i) are the results for $T_f = 168$ h.

https://doi.org/10.5194/egusphere-2025-1785
Preprint. Discussion started: 30 April 2025

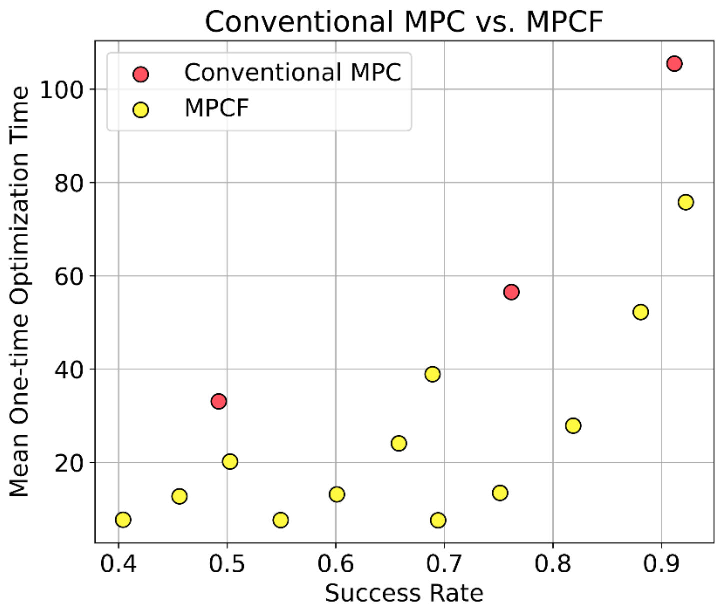

Figure 5: Comparison between the conventional MPC (i.e., $T_\mathrm{p} = T_\mathrm{f}$) and the MPCF (i.e., $T_\mathrm{p} < T_\mathrm{f}$) using the results for $T_\mathrm{c} = 6$ h. The horizontal axis is the success rate (SR), and the vertical axis is the mean one-time optimization time (MOOT). The red dots indicate the conventional MPC, and the yellow dots indicate the MPCF.

4.3 Sensitivity to the constrained norm of the control input

This experiment investigates the sensitivity to the constrained norm of the control input U_max. The placement of the control input is X_{i-1}, X_i, and X_{i+1} as in Sect. 4.2. The setting of the control, prediction, and foreseeing horizons is $T_\mathrm{c} = 6$ h, $T_\mathrm{p} = 24$ h, and $T_\mathrm{f} = 96$ h, respectively. To investigate the sensitivity, the constrained norm of the control input U_max is set to $U_\mathrm{max} =$ 1.0, 2.0, 4.0, 7.0, and 14. Recall that the value of the norm of the control input corresponds to the temporal rate of change of the state $\mathrm{d}X_i/\mathrm{d}t$ and therefore cannot be directly compared to the value of the state X_i.

The results are shown in Fig. 6. Increasing U_max improves the SR (Fig. 6, a). In particular, SR $= 0.99$ is achieved at $U_\mathrm{max} = 14$ under this setting. Here, $\|\boldsymbol{u}\| = 14$ corresponds approximately to the magnitude of the control input with a magnitude coefficient $\alpha = 0.7$ in the approach of Sun et al. (2023), and is not regarded as a large value compared to the previous study. For all values of U_max, the MMCI is correctly constrained to U_max (Fig. 6, b). On the other hand, the MOOT increases with increasing U_max (Fig. 6, c). We speculate that this is due to the expanded search range for optimizing the control inputs resulting from the increase in U_max.

https://doi.org/10.5194/egusphere-2025-1785
Preprint. Discussion started: 30 April 2025

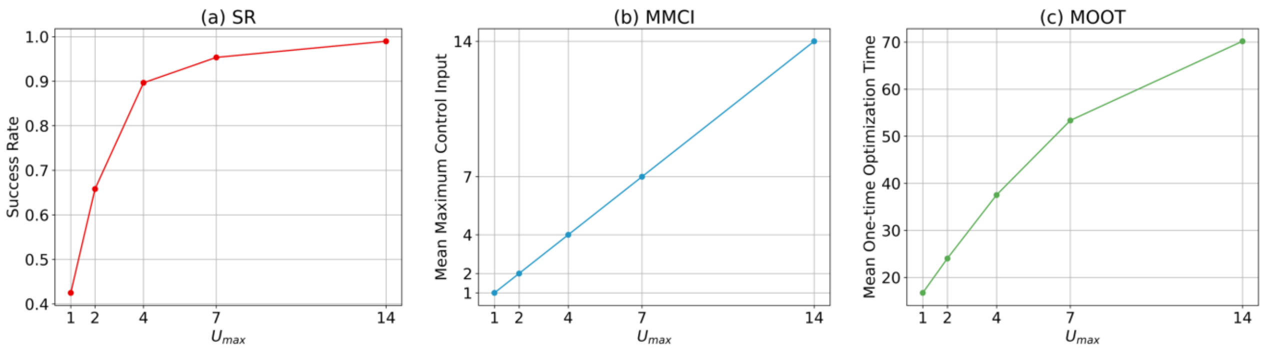

Figure 6: Sensitivity to the constrained norm of the control input $U_{\max}$ with three indicators: (a) the success rate (SR), (b) the mean maximum control input (MMCI), and (c) the mean one-time optimization time (MOOT). The horizontal axis of all plots is $U_{\max}$. The vertical axes in (a), (b), and (c) are the SR, MMCI, and MOOT, respectively.

4.4 Sensitivity to the placement of the control input

Sun et al. (2023), conducting CSEs with the L96, demonstrated the effectiveness of adding control inputs to sites around extreme events rather than to random sites. To deepen this discussion further, this study explores the sensitivity to the placement of the control input. The setting of the control, prediction, and foreseeing horizons, T_c, T_p, and T_f, respectively, is identical to the previous experiment in Sects. 4.1 and 4.3 ($T_c = 6$ h, $T_p = 24$ h, and $T_f = 96$ h). The setting of the constrained norm of the control inputs $U_{\max}$ is the same as in the previous experiment in Sect. 4.2 (i.e., $U_{\max} = 2.0$). To examine the sensitivity, there are two settings with respect to the placement of the control input. In the first setting, a one-variable control input is placed at X_{i-2}, X_{i-1}, X_i, X_{i+1}, or X_{i+2}. In the second setting, three-variable control inputs are placed at $(X_{i-3}, X_{i-2}, X_{i-1})$, (X_{i-2}, X_{i-1}, X_i), (X_{i-1}, X_i, X_{i+1}), (X_i, X_{i+1}, X_{i+2}), or $(X_{i+1}, X_{i+2}, X_{i+3})$. Note that this study defines the direction of X_i, X_{i+1}, X_{i+2}, ... as eastward and the direction of X_i, X_{i-1}, X_{i-2}, ... as westward in the L96.

The results for the one-variable control input are shown in Fig. 7 (a−c). The SR is highest when the control input is added at X_i, suggesting that adding the control input directly to the grid point of an extreme event is more efficient than adding it to surrounding grid points. In addition, the SR tends to be higher when the control input is added to the western side rather than the eastern side. Here, the phase velocity and group velocity of the L96 model are generally known to be westward and eastward, respectively, with a forcing parameter $F = 8.0$ (Lorenz and Emanuel, 1998). Additionally, the group velocity is typically interpreted as the velocity of energy propagation (Whitham, 1974). Therefore, this result implies that the upstream side of the energy propagation (i.e., western side: X_{i-1}, X_{i-2}, ...) is more effective in controlling X_i than simply the upstream side of the wave (i.e., the eastern side: X_{i+1}, X_{i+2}, ...). In addition, the lowest MOOT is indicated when the control input is added to X_i (Fig. 7, c) when the highest SR is achieved (Fig. 7, a). The norm of the control input is correctly constrained to $U_{\max}$ in all cases, as shown in Fig. 7 (b).

https://doi.org/10.5194/egusphere-2025-1785
Preprint. Discussion started: 30 April 2025

The results of the three-variable control inputs are shown in Fig. 7 (d−f). As shown in Fig. 7 (d), the SR is higher in the case including X_i: (X_{i-2}, X_{i-1}, X_i), (X_{i-1}, X_i, X_{i+1}), and (X_i, X_{i+1}, X_{i+2}). In addition, by comparing the cases without X_i: $(X_{i-3}, X_{i-2}, X_{i-1})$ and $(X_{i+1}, X_{i+2}, X_{i+3})$, the SR is higher on the upstream side of the energy propagation. These results are consistent with the previous result for the one-variable control input. In addition, because the degrees of freedom are increased by the three control inputs, the overall SR improves compared to the case with the one-variable control input. On the other hand, the MOOT exhibits a different behavior from the previous result of the one-variable control input, as shown in Fig. 7 (f). There is no significant difference in the MOOT overall, but it is slightly lower on the east side. The detailed reason for this is unclear since optimization becomes more complicated when the control inputs consist of three variables. Even with the three-variable control inputs, the norm of the control input is correctly constrained to $U_{\max}$ (Fig. 7, e).

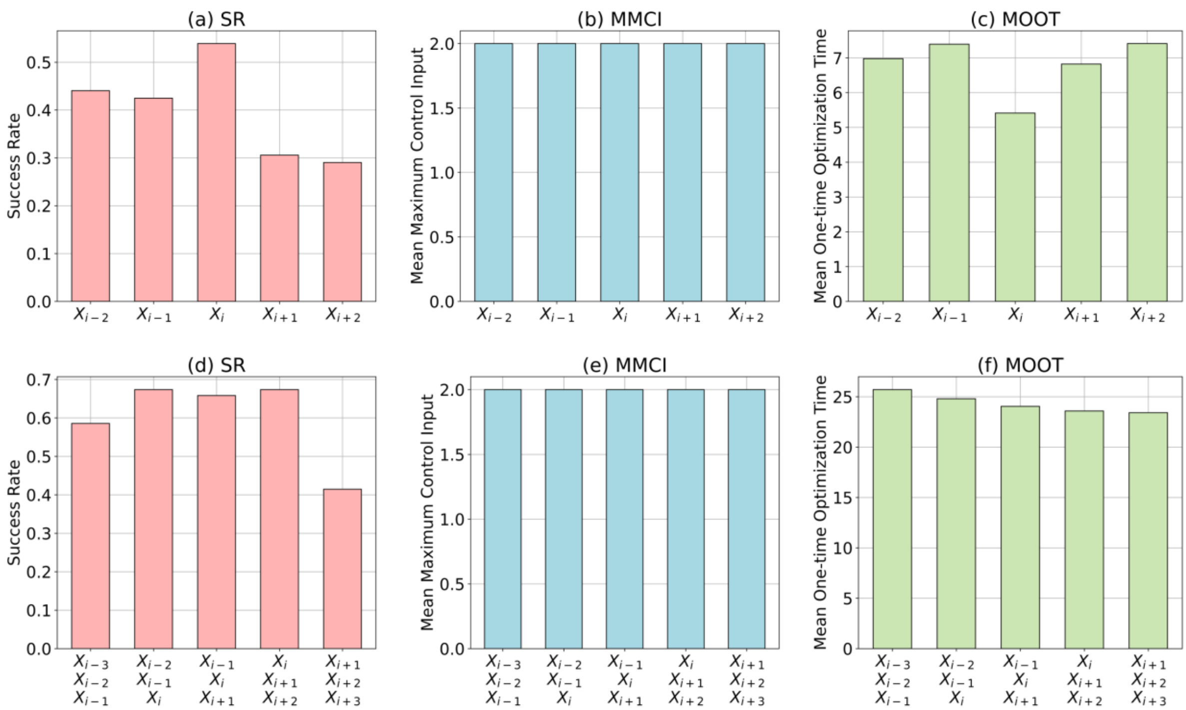

Figure 7: Sensitivity to the placement of the control input with three indicators: the success rate (SR), the mean maximum control input (MMCI), and the mean one-time optimization time (MOOT). (a−c) are the results of adding control inputs to X_{i-2}, X_{i-1}, X_i, X_{i+1}, or X_{i+2}. (d−f) are the results of adding control inputs to $(X_{i-3}, X_{i-2}, X_{i-1})$, (X_{i-2}, X_{i-1}, X_i), (X_{i-1}, X_i, X_{i+1}), (X_i, X_{i+1}, X_{i+2}), or $(X_{i+1}, X_{i+2}, X_{i+3})$.

5 Conclusion

This study proposed the MPCF, a framework incorporating the novel concept of the foreseeing horizon into the conventional MPC, designed to mitigate extreme events in chaotic dynamical systems. By introducing the foreseeing horizon, the MPCF

https://doi.org/10.5194/egusphere-2025-1785
Preprint. Discussion started: 30 April 2025

successfully reduced the computational cost of optimization for identifying the control inputs. That is, the MPCF partially overcame low rapidity, which is a limitation of the conventional MPC. This improvement may be attributed to the earlier detection of extreme events and the utilization of the sensitivity to initial conditions of chaotic dynamical systems.

The effectiveness of the MPCF was demonstrated through sensitivity experiments on several parameters in the CSEs with the L96. Specifically, our experiment in Sect. 4.2 showed that introducing the foreseeing horizon T_{f} improved the SR without significantly increasing the MOOT when the control horizon T_{c} is short, rather than extending the control horizon T_{c} or prediction horizon T_{p}. In addition, by comparing the MPCF with the conventional MPC using the results for $T_{\mathrm{c}} = 6$ h, it was shown that the MPCF achieved almost equivalent SRs to the conventional MPC with lower MOOTs. Our experiment in Sect. 4.3 demonstrated that increasing the constrained norm of the control input $U_{\max}$ improved the SR with an associated increase in the MOOT. Our experiment in Sect. 4.4 showed that strategically placing the control input at the grid point where the extreme event occurs and at the upstream side of the energy propagation is beneficial. In conclusion, the MPCF is a promising control framework that effectively balances the optimality, restrictiveness, and rapidity for mitigating extreme events in chaotic dynamical systems.

This study provided steady progress with the L96 as the second phase in a series of studies applying MPC to CSE following Kawasaki and Kotsuki (2024), which used the Lorenz 63 model. However, further investigations in mathematical weather control approaches are required to realize weather control aimed at mitigating extreme events. This study highlights the rapidity of MPC, but that achieved only by the MPCF may be insufficient for weather control applications, which require extremely high computational costs. Therefore, exploring additional strategies to further accelerate the rapidity of MPC is essential, such as integrating AI into weather prediction models. Additionally, while this study only conducted the idealized experiments that ignored uncertainties induced by numerical models and actual interventions, we need to investigate the influence of such errors and imperfections. Finally, experiments with realistic NWP models that have multiple spatial dimensions and physical quantities are indispensable for detailed discussions of weather control feasibility. Such experiments would enable a more comprehensive evaluation of MPC under realistic atmospheric conditions.

Appendix A: The initial state used in optimization and the reference trajectory

This appendix describes how to select the initial state used in optimization and the reference trajectory for the MPCF in this study. We begin by explaining the selection of the initial state. The critical issue is that the NR cannot be used as the initial state for optimizing the control inputs because the true state of the system is unknown. Therefore, an analysis ensemble member is used as the initial state instead of the NR. The choice of which analysis ensemble member to select as the initial state has already been discussed in Kawasaki and Kotsuki (2024). This study employs the ensemble member exhibiting the largest extreme event within the ensemble forecast, based on Kawasaki and Kotsuki (2024). For example, assuming ensemble forecasts as shown in Fig. A1, ensemble member A is selected as the initial state because it exhibits the largest extreme event within the ensemble forecast.

https://doi.org/10.5194/egusphere-2025-1785
Preprint. Discussion started: 30 April 2025

We then explain how to select the reference trajectory for the MPCF in this study. The reference trajectory provides a guiding trajectory to lead the NR to a non-disastrous regime. Therefore, ensemble members indicating extreme events are excluded from the reference trajectory candidates. For example, assuming ensemble forecasts as shown in Fig. A1 again, ensemble members A and D are not selected as the reference trajectory. Among the remaining candidates, the ensemble member with the smallest value at time $t_{\mathrm{ext-max}}$ showing the maximum extreme event (i.e., ensemble member C) is selected as the reference trajectory in this study. This is because our preliminary experiments with several potential reference trajectory options demonstrated that the option—selecting ensemble member C in Fig. A1—gave the best results in terms of the SR. If all ensemble members show extreme events, the ensemble forecast is performed again at the previous observation time (i.e., 6 h earlier). If a non-disastrous ensemble member is not found at the previous observation time, go back to the earlier observation time until a non-disastrous ensemble member is found. If a non-disastrous ensemble member is not found after going back to the starting point of the CSE, the CSE is terminated as a failure.

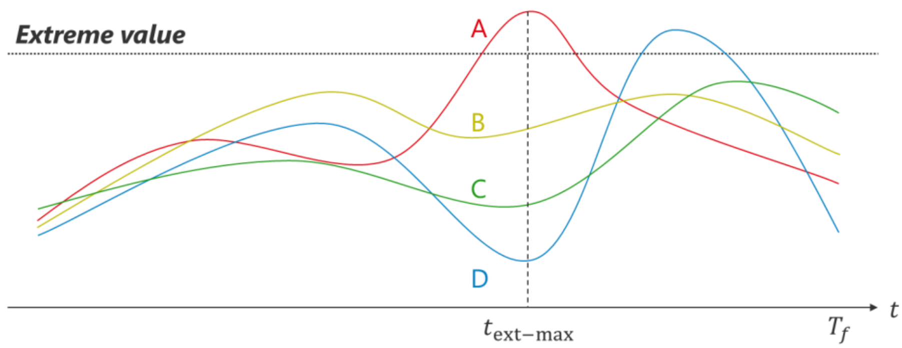

Figure A1: An example of ensemble forecasts to describe how to select the initial state used in optimization and the reference trajectory for the MPCF in this study. Ensemble member A (red solid line) indicates the largest extreme event (black dotted line) within the ensemble forecast at $t_{\mathrm{ext-max}}$. In this study, ensemble member A is employed as the initial state of the optimization. Ensemble member B (blue solid line) shows the second largest value at $t_{\mathrm{ext-max}}$ without extreme events. Ensemble member C (green solid line) represents the smallest value at $t_{\mathrm{ext-max}}$ among the ensemble members without extreme events. Ensemble member C is therefore employed as the reference trajectory in this study. Ensemble member D (blue solid line) indicates the smallest value at $t_{\mathrm{ext-max}}$ among all ensemble members. However, ensemble member D is not selected as the reference trajectory because it predicts an extreme event later.

Code availability. The code that supports the findings of this paper is available from the corresponding author upon reasonable request. In addition, all the codes used in this study are stored for five years at Chiba University.

Data availability. The authors declare that all data supporting the findings of this paper are available within the figures and tables of this paper.

Author contribution. FK, AO, TT, KK, and SK conceptualized this study. FK conducted all experiments and wrote the manuscript. All authors contributed to framing and revising the paper substantially. AO and SK supervised and directed this study.

Competing interests. The authors declare that they have no conflict of interest.

Acknowledgements. The authors thank Drs. Daisuke Hotta of Meteorological Research Institute and Keita Tokuda of Juntendo University for valuable discussion and information.

Financial support. This study was supported by JST SPRING (Grant Number JPMJSP2109), JST Moonshot R&D program (Grant Number JPMJMS2389), the Japan Society for the Promotion of Science (JSPS) via KAKENHI (Grant Numbers JP21H04571 and JP25H00752), and the IAAR Research Support Program of Chiba University.

References

Bloom, S. C., Takacs, L. L., Silva, A. M. da, and Ledvina, D.: Data Assimilation Using Incremental Analysis Updates, Monthly Weather Review, 124, 1256–1271, https://doi.org/10.1175/1520-0493(1996)124<1256:DAUIAU>2.0.CO;2, 1996.

Burgers, G., Leeuwen, P. J. van, and Evensen, G.: Analysis Scheme in the Ensemble Kalman Filter, Monthly Weather Review, 126, 1719–1724, https://doi.org/10.1175/1520-0493(1998)126<1719:ASITEK>2.0.CO;2, 1998.

Dimet, F.-X. L. and Talagrand, O.: Variational algorithms for analysis and assimilation of meteorological observations: theoretical aspects, Tellus A, 38A, 97–110, https://doi.org/10.1111/j.1600-0870.1986.tb00459.x, 1986.

Evensen, G.: Sequential data assimilation with a nonlinear quasi-geostrophic model using Monte Carlo methods to forecast error statistics, Journal of Geophysical Research: Oceans, 99, 10143–10162, https://doi.org/10.1029/94JC00572, 1994.

Kawasaki, F. and Kotsuki, S.: Leading the Lorenz-63 system toward the prescribed regime by model predictive control coupled with data assimilation, Nonlinear Processes in Geophysics Discussions, 1–22, https://doi.org/10.5194/npg-2024-4, 2024.

Kotsuki, S.: Exploring weather control technology to steer the atmosphere towards favorable directions based on ensemble data assimilation, AGU24, 2024.

Lawson, W. G. and Hansen, J. A.: Implications of Stochastic and Deterministic Filters as Ensemble-Based Data Assimilation Methods in Varying Regimes of Error Growth, Monthly Weather Review, 132, 1966–1981, https://doi.org/10.1175/1520-0493(2004)132<1966:IOSADF>2.0.CO;2, 2004.

Liu, C., Xiao, Q., and Wang, B.: An Ensemble-Based Four-Dimensional Variational Data Assimilation Scheme. Part I: Technical Formulation and Preliminary Test, Monthly Weather Review, 136, 3363–3373, https://doi.org/10.1175/2008MWR2312.1, 2008.

https://doi.org/10.5194/egusphere-2025-1785
Preprint. Discussion started: 30 April 2025

Lorenz, E. N.: Deterministic Nonperiodic Flow, Journal of the Atmospheric Sciences, 20, 130–141, https://doi.org/10.1175/1520-0469(1963)020<0130:DNF>2.0.CO;2, 1963.

Lorenz, E. N.: Predictability: a problem partly solved, Proc, Seminar on Predictability, Seminar on Predictability, Reading, 4-8 September 1995, ECMWF, 1-18, https://www.ecmwf.int/en/elibrary/75462-predictability-problem-partly-solved, 1996.

Lorenz, E. N. and Emanuel, K. A.: Optimal Sites for Supplementary Weather Observations: Simulation with a Small Model, Journal of the Atmospheric Sciences, 55, 399–414, https://doi.org/10.1175/1520-0469(1998)055<0399:OSFSWO>2.0.CO;2, 1998.

Miyoshi, T. and Sun, Q.: Control simulation experiment with Lorenz's butterfly attractor, Nonlin. Processes Geophys., 29, 133–139, https://doi.org/10.5194/npg-29-133-2022, 2022.

Ouyang, M., Tokuda, K., and Kotsuki, S.: Reducing manipulations in a control simulation experiment based on instability vectors with the Lorenz-63 model, Nonlinear Processes in Geophysics, 30, 183–193, https://doi.org/10.5194/npg-30-183-2023, 2023.

Sasaki, Y.: Proposed Inclusion of Time . Variation Terms, Observational and Theoretical, in Numerical Variational Objective Analysis, Journal of the Meteorological Society of Japan, 47, 115–124, https://doi.org/10.2151/jmsj1965.47.2_115, 1969.

Sasaki, Y.: SOME BASIC FORMALISMS IN NUMERICAL VARIATIONAL ANALYSIS, Monthly Weather Review, 98, 875–883, https://doi.org/10.1175/1520-0493(1970)098<0875:SBFINV>2.3.CO;2, 1970.

Sawada, Y.: Ensemble Kalman Filter Meets Model Predictive Control in Chaotic Systems, Sola, 20, 400–407, https://doi.org/10.2151/sola.2024-053, 2024.

Sun, Q., Miyoshi, T., and Richard, S.: Control simulation experiments of extreme events with the Lorenz-96 model, Nonlinear Processes in Geophysics, 30, 117–128, https://doi.org/10.5194/npg-30-117-2023, 2023.

Talagrand, O. and Courtier, P.: Variational Assimilation of Meteorological Observations With the Adjoint Vorticity Equation. I: Theory, Quarterly Journal of the Royal Meteorological Society, 113, 1311–1328, https://doi.org/10.1002/qj.49711347812, 1987.

Thompson, P. D.: Reduction of Analysis Error Through Constraints of Dynamical Consistency, Journal of Applied Meteorology and Climatology, 8, 738–742, https://doi.org/10.1175/1520-0450(1969)008<0738:ROAETC>2.0.CO;2, 1969.

Tsuyuki, T. and Miyoshi, T.: Recent Progress of Data Assimilation Methods in Meteorology, Journal of the Meteorological Society of Japan. Ser. II, 85B, 331–361, https://doi.org/10.2151/jmsj.85B.331, 2007.

Whitham, G. B.: Linear and nonlinear waves, Wiley, New York, 636 pp., 1974.

Zupanski, M.: Maximum Likelihood Ensemble Filter: Theoretical Aspects, Monthly Weather Review, 133, 1710–1726, https://doi.org/10.1175/MWR2946.1, 2005.